

In-Situ Thermoreversible Gelation of Block and Star Copolymers of Poly(ethylene glycol) and Poly(*N*-isopropylacrylamide) of Varying Architectures

Hai-Hui Lin and Yu-Ling Cheng*

Department of Chemical Engineering and Applied Chemistry, University of Toronto, Toronto, Ontario, M5S 3E5 Canada

Received October 27, 2000; Revised Manuscript Received March 8, 2001

ABSTRACT: We report the development of a new gelation mechanism and a new family of polymers that self-assembles to form gels in a thermoreversible fashion. The polymers are block or star copolymers with a central hydrophilic poly(ethylene glycol) (PEG) segment (A) and temperature responsive poly(*N*-isopropylacrylamide) (PNIPAAm) terminal segments (B). Copolymers of various architectures, AB, A(B)₂, A(B)₄, and A(B)₈, were synthesized to investigate the structures and properties relationship. At 5 °C, the viscosities of 20 wt % solutions were between 700 and 950 cP, and they could be easily injected through a 25 G needle. Upon warming to body temperature, A(B)₂, A(B)₄, and A(B)₈ formed a strong associative network gel with aggregates of PNIPAAm segments acting as physical cross-links, whereas AB formed a weaker gel by micellar packing and entanglement. The values of elastic modulus, loss tangent, and yield strength were 1000–2500 Pa, 0.24–0.62, and 200–860 Pa, respectively. The gelation kinetic was fast; a typical gelation time for a solution of 5 mL in volume was less than a minute. No significant syneresis was observed after 2 months at 37 °C. DSC results indicated that the thermal behavior of material was completely reversible even after 30 heat-and-cool cycles. These materials are promising candidates for in-situ gelation applications such as injectable drug delivery, tissue engineering scaffolds, and anatomical barriers.

Introduction

Self-assembling hydrogels have been receiving increasing attention in the past few years, both for their intrinsic scientific interest and for their potential clinical and nonclinical applications. A number of elegant mechanisms for self-assembling hydrogels have been proposed. DeJong et al. reported gels formed by stereocomplexation between L-lactic acid and D-lactic acid chains grafted on dextran molecules. The stereocomplex melts reversibly when heated from 20 to 80 °C with no distinct melting temperature.¹ Nagahara and Matsuda showed that gels can be formed by complexation between complementary oligonucleotides grafted onto hydrophilic polymers.² Miyata et al. prepared antigen-sensitive hydrogels based on antigen–antibody binding.^{3,4} Petka et al. illustrated a gelation mechanism using triblock copolymers containing a central hydrophilic core and terminal leucine zipper peptide domains. The terminal domains form coil–coil dimers or higher order aggregates to provide cross-linking when cooled from above its pH-dependent melting point. Thermoreversibility was demonstrated with some hysteresis due to the slow kinetics of coil–coil interactions.⁵ Another family of peptide-based self-assembling gels reported by Cappello et al. consist of block copolymers that contain repeating amino sequences from silk and elastin proteins.⁶ Gelation occurs via a hydrogen-bond-mediated chain crystallization mechanism when heated to body temperature. The gelation process is not completely reversible, and the gelation occurs over a relatively long time scale of more than 25 min. A group led by Kim have reported the development of thermosensitive biodegradable hydrogels that self-assemble and form gels

via a micellar aggregation mechanism:^{7–10} the micelles consisting of hydrophobic cores and hydrophilic coronas. They have made diblock and triblock copolymers of poly(ethylene glycol) (PEG) and either poly(L-lactic acid) (PLLA) or poly(lactide-*co*-glycolide) (PLGA). The triblock copolymers synthesized have PEG segments on the two ends to facilitate micelle formation, e.g., PEG-PLGA-PEG. Upon heating, the copolymers in water were shown to undergo fluid-to-gel transitions, followed by gel-to-fluid transitions at even higher temperatures. Gel formation is believed to occur via growth and aggregation of micelles, while the gel-to-fluid transition at higher temperatures is thought to be due to breakage of micelle structure. These gels are distinct in their optical transparency—an indication of the small size of the micellar aggregates. Of particular interest are diblock copolymers PEG–PLGA and triblock copolymers PEG–PLGA–PEG that transform from aqueous solutions into gels at 20 °C to transition temperatures between about 20 and 40 °C depending on polymer composition and concentration.^{7–9} Micellar aggregation-induced thermoreversible gelation has also been observed in other polymer solutions, most notably the commercially available family of triblock copolymers of ethylene oxide and propylene oxide, PEO–PPO–PEO.^{11,12}

Among the self-assembling gels reported to date, those that form liquid aqueous solutions at ambient conditions but gel upon contact with physiologic conditions, i.e., PEG–PLGA, PEG–PLGA–PEG, and the silk and elastin sequence based peptides, are of particular interest. The in-situ gelation property can be exploited in many clinical applications, including injectable drug delivery and anatomical barriers, and can be used as a gentle means of cell encapsulation. While not truly a gelation process, solvent-exchange-induced precipitation of polymers has also been exploited as a mechanism for

* Corresponding author. Phone 416-978-5500; Fax 416-978-8605; e-mail ylc@chem-eng.toronto.edu.

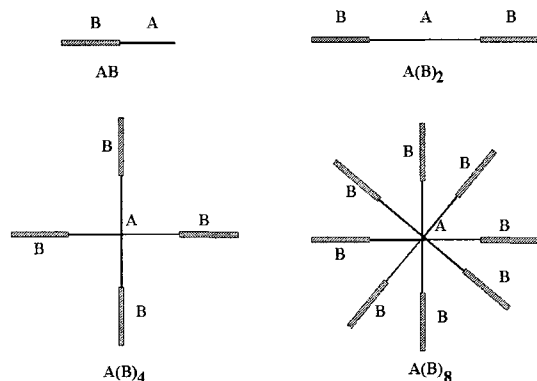


Figure 1. Schematic diagram of AB, A(B)₂, A(B)₄, and A(B)₈ copolymers.

producing in-situ “gellable” materials.^{13,14} After administration of a polymer dissolved in a nonaqueous solvent, the exchange of the solvent with water in the physiologic environment results in the precipitation of the polymer, forming a solid mass in situ.

In this paper, we report the development of a new gelation mechanism and a new family of polymers that self-assembles to form gels in a thermoreversible fashion. The polymers are of a general form that includes a central hydrophilic polymer segment A and more than one terminal segment B. The central segment A is chosen such that a homopolymer of A would remain soluble in water throughout the temperature range of interest. The terminal segment B is selected to be a polymer that shows a lower critical solution temperature (LCST) within the temperature range of interest; thus, a homopolymer of B would be soluble in water at low temperatures and precipitate or aggregate with other homopolymers of B at above LCST. It is hypothesized that block copolymers of such compositions and such molecular architectures would then form liquid solutions in water at below the LCST of B and, upon heating, form gels via the agglomeration of B segments. The B aggregates formed would be covalently joined by A segments; thus, the B aggregates would represent physical cross-links that connect solvated A segments in a true three-dimensional gel network.

In this study, poly(ethylene glycol) (PEG) is selected as a model unresponsive hydrophilic segment A, and poly(*N*-isopropylacrylamide) or PNIPAAm is selected to be the responsive polymer segment B. PNIPAAm is known to exhibit a lower critical solution temperature at about 32 °C. Below the LCST, PNIPAAm dissolves readily in water but forms aggregates and precipitates when heated above its LCST. We report the synthesis, gelation characteristics, and rheological properties of 2-arm, 4-arm, and 8-arm block copolymers of PEG and PNIPAAm (Figure 1). The one-arm diblock copolymer PEG-*b*-PNIPAAm is also investigated for comparison. It is expected that the diblock copolymer would gel via a micellar aggregation mechanism rather than a physical cross-linking mechanism. Other studies of PEG-PNIPAAm copolymers of various architectures have been reported,^{15–20} including PEG-PNIPAAm-PEG triblocks, PNIPAAm-*co*-NASI-*co*-PEG loosely cross-linked networks, and PNIPAAm-*g*-PEG. None focused on the same molecular architectures as the ones selected for this study, and none were designed and synthesized with in-situ gelation applications in mind.

Experimental Method

The copolymers were synthesized by Ce⁴⁺/OH redox initiated free radical polymerization in water. Four hydroxyl-terminated PEG's were purchased from Shearwater and used without further purification: monomethoxy-PEG of 2000 Da (i.e., 1-arm of length 2000 Da), linear PEG diol of 4600 Da (i.e., 2-arm PEG with each arm length of 2300 Da), 4-arm star PEG of 9300 Da (arm length = 2325 Da), and 8-arm star PEG of 19 700 Da (arm length = 2460 Da). The star PEGs were synthesized by cross-linking monodispersed linear PEGs at one end with divinylbenzene or by ethoxylation of various polyols;²¹ the resulting functionalized PEG's have polydispersity indices of less than 1.04. To prevent oxidative degradation as well as hydrolysis, the PEGs were capped under dry helium blanket and stored at below –10 °C. NIPAAm monomer (Acros, 99% stabilized with 0.1% MHQ) was first double recrystallized in 50/50 heptane/toluene solvent and recovered by vacuum filtration. The recovered solid was then redissolved in distilled deionized water and filtered through an anionic exchange resin [IRA-402, Cl[–] form, Supelco] to remove trace acrylic acid. The purified NIPAAm was recovered by freeze-drying at –55 °C. The 0.4 M Ce⁴⁺ solutions were prepared by dissolving ceric ammonium nitrate [Sigma, 99%] in distilled deionized water. The solutions were either prepared just prior to use or sonicated to remove dissolved oxygen and stored for a short time at 5 °C in tightly capped high-density polyethylene vials prior to use.

Copolymer synthesis was carried out by first dissolving PEG and NIPAAm at appropriate feed ratios in water and then adding a 0.4 M Ce⁴⁺ solution. The mixture was then sonicated to remove dissolved oxygen. The reaction was carried out in polypropylene vials under water-saturated helium blanket at 30 °C for 24 h. Glassware was not used during synthesis to avoid initiation by Ce⁴⁺/glass surface OH groups. A typical reaction batch consisted of 1.5 g of PEG, 0.5 g of NIPAAm, and 4 mL of 0.4 M Ce⁴⁺ solution, with a total solution volume of 15 mL.

The main mechanism of producing PNIPAAm homopolymer in this reacting system is believed to be the direct initiation of monomers by Ce⁴⁺.²² Reaction conditions were selected to ensure that the final product was low in PNIPAAm homopolymer. For the conditions used, if no OH groups are present, less than 10% NIPAAm was initiated. On the other hand, if OH groups are present (i.e., PEG present), the conversion was greater than 90%. Therefore, it was concluded that, in the worst scenario, if Ce⁴⁺ initiation of OH groups and NIPAAm monomers are equal, then only 1 out of 9 reacted monomers would be part of a homopolymer. Given that OH groups are the preferential target of Ce⁴⁺, it is expected that in the presence of PEG the fraction of monomers that react to form homopolymer should be minimal.

The 1-arm and 2-arm copolymers were purified by dialysis using cellulose ester tubing with MWCO of 3500 and 8000, respectively [Fisher Scientific]. The 4-arm and 8-arm copolymers were purified by size exclusion gel chromatography using a gravity-feed column 200 mL in volume and 15 cm in height, packed with Sephacryl beads [S-200 HR, Supelco]. The copolymers were then recovered from the aqueous solution by freeze-drying at –55 °C. The purified copolymers were in white powder form, and their solutions were colorless. Using Ce⁴⁺ as a colorimetric reagent, no unreacted OH groups were detected.²³ This assay was used as an indication that the final product was free of PEG homopolymer contamination.

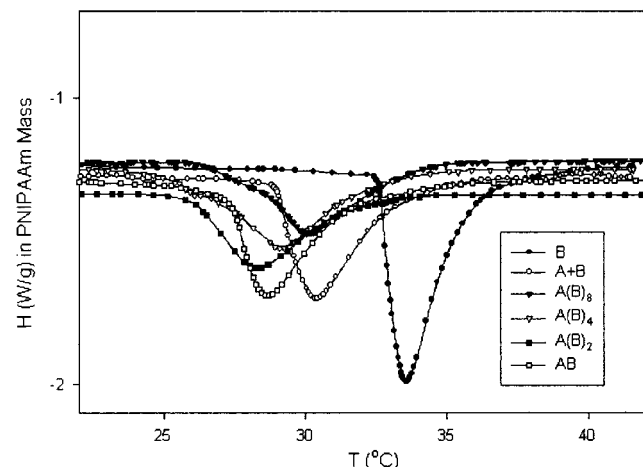
The copolymer molecular weights were determined by proton NMR [Varian Unity Plus 500 MHz]. The ratio of the methyl protons in isopropyl groups to the methylene protons of PEG's was used to determine the ratio of NIPAAm to ethylene glycol repeat units. Using the known molecular weight of PEG, the molecular weight of PNIPAAm segments and thus the copolymer molecular weight can be deduced.

The thermal characteristics of the copolymers were determined by running DSC [TA2010, TA Instrument] scans of 20 wt % aqueous solutions of each of the copolymers at a heating rate of 2 °C/min. Transition temperatures (i.e., both onset and

Table 1. Composition of Copolymers

structures	A block weight ^a (Da)	PEG MW per arm (Da)	B block weight (Da) ^{b,c}	PEG/PNIPAm (by wt)	total mol wt (Da) ^c
AB	2000	2000	2200 ± 200	48/52	4400 ± 200
A(B) ₂	4600	2300	1900 ± 200	55/45	8400 ± 400
A(B) ₄	9300	2330	2100 ± 200	52/48	17 700 ± 800
A(B) ₈	19 700	2460	2400 ± 200	51/49	39 000 ± 1600

^a As reported by manufacturer; polydispersity of 1.04 or better. ^b Average from three synthesis batches. ^c As calculated from NMR analysis.

**Figure 2.** Endotherm of AB, A(B)₂, A(B)₄, and A(B)₈.

peak temperature of endotherm) and enthalpies were measured. The mechanical and rheological properties of the copolymers were characterized using a temperature-controlled rheometer [Carri-Med, TA Instrument] with a cone and plate (4 cm diameter, 2° angle) geometry. Yield stress (σ_y), critical strain (γ_c), and the elastic and loss moduli (G' , G'') were determined under oscillatory mode at 37 °C. Solution viscosities were measured under flow mode at 5 °C using 20 wt % copolymer solutions in water.

Results and Discussion

Table 1 shows the molecular weights of the copolymers and the blocks within the copolymers as determined by proton NMR. Since the PEGs used in this case are essentially monodispersed, the molecular weight calculated based on the mole ratio of PEG and PNIPAm subunits can be taken as the number-averaged molecular weight, M_n . Because of various technical difficulties in measuring weight-averaged molecular weight, M_w , the molecular weight distribution of samples is not reported in this paper. However, due to the very nature of free radical polymerization and batch-mode synthesis, the copolymers are likely to be polydispersed. According to the NMR results, all the copolymers have approximately a one-to-one weight ratio of PEG to PNIPAm—a result predetermined by the choice of PNIPAm to PEG ratio during synthesis. The molecular weight per “arm” for each of the copolymers is also approximately constant; each arm consists of a PEG segment and a PNIPAm segment, with a total arm molecular weight of approximately 4000–4500. Thus, the multiarmed copolymers can be viewed simplistically as a number of one-armed copolymers (AB) joined at their A ends (Figure 1).

The DSC scans of all the copolymers showed endothermic transitions (Figure 2) upon heating. The transition temperatures (i.e., using the peak temperature of endotherm) of the copolymers measured upon heating are in the range 28–30 °C, 3–5 °C lower than that of PNIPAm homopolymer, 33.6 °C. (Table 2). However,

Table 2. Transition Temperature and Enthalpy Change^a

structure	transition temp (°C)		enthalpy change (J/g PNIPAm)
	T_{onset}	T_{peak}	
B	32.6 ± 0.2	33.6 ± 0.2	43 ± 2
A + B	29.1 ± 0.2	30.4 ± 0.2	34 ± 2
AB	27.3 ± 0.2	28.7 ± 0.2	30 ± 2
A(B) ₂	26.4 ± 0.2	28.5 ± 0.2	29 ± 2
A(B) ₄	26.2 ± 0.2	29.3 ± 0.2	29 ± 2
A(B) ₈	28.2 ± 0.2	30.3 ± 0.2	28 ± 2

^a All samples were prepared as 20 wt % aqueous solutions, heating at a rate of 2 °C/min. B is PNIPAm homopolymer with a molecular weight of 12 000 Da, also prepared as 20 wt % solution. A + B is a 10 wt %–10 wt % blend of 2000 Da PEG and 12 000 Da PNIPAm homopolymer in water. Both onset and peak temperatures of endotherm are tabulated.

the range of transition temperature of copolymers is comparable to that of a 50/50 PEG/PNIPAm homopolymer blend, which is 30.4 °C (Table 2). The thermodynamic basis for LCST depression is clear. Materials that exhibit LCST must have a negative entropy of mixing. To depress the LCST, an additive has to make the entropy of mixing even more negative, which then makes ΔG_{mix} more positive. In molecular terms, the additive (PEG in this case) can make the entropy of mixing more negative and depress the LCST if it causes an ordering of water molecules, i.e., if it creates structure in the water or that it makes the water more icelike. On the one hand, if the additive is chaotropic and break the water–water hydrogen bonds, an elevation of LCST will result. Although the thermodynamic principles are clear, why PEG coils appear to have a water-structure creation effect is not yet clear to us.

The endothermic enthalpy changes at the transition temperatures normalized on a PNIPAm weight basis ranged from 28 to 30 J/g for the copolymers, lower than the 43 J/g seen for PNIPAm homopolymer (Table 2). The range of ΔH values suggests that the copolymer molecular architecture influences the phase transition of the PNIPAm segments, while the comparison between the copolymers and the homopolymer suggests that the presence of PEG may prevent PNIPAm segments from fully collapsing. The samples were also subjected to cyclic heating and cooling for up to 30 cycles. Figure 3 shows the superposition of the DSC scans for multiple cycles; the superposability of the scans indicates that the gelation process is completely reversible. There is a difference, however, between the cooling curve and the heating curve. Although the enthalpy of gel melting is identical to the enthalpy of gel formation, at a heating/cooling rate of 2 °C/min, there is a difference between the peak temperatures of the heating endotherm and the cooling exotherm, 2.0 °C in the example shown in Figure 3. The difference may be attributed to the kinetics of gelation process. At infinitely slow cooling/heating rates, the two peak temperatures should be identical.²⁴ The relatively small temperature lag seen with these copolymers is indicative of rapid gelation kinetics. Another thermoreversible

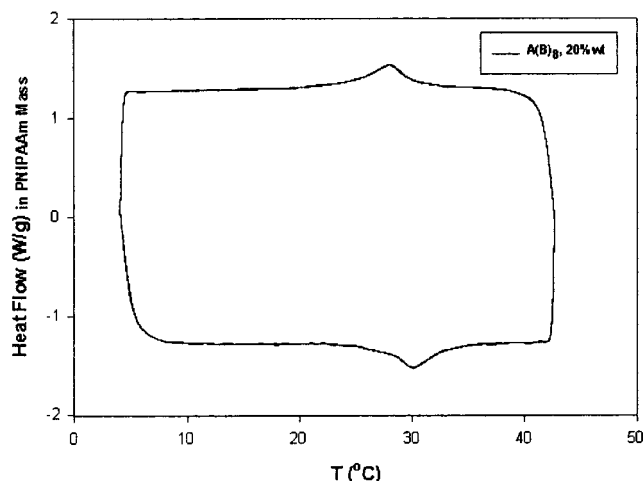


Figure 3. Cyclic heating and cooling of A(B)₈.

polymer hydroxypropylmethylcellulose (HPC) has been reported to have a temperature lag of 8–10 °C at a much slower heating rate of 0.25 °C/min.²⁴

The thermal transitions detected by DSC correspond to visible phase transitions. Below the transition temperatures, aqueous copolymer solutions are liquids that flow easily (Figure 4A). As the solutions are heated to above the transition temperature, they rapidly transform into gels of considerable strength (Figure 4B). A range of physical properties may be achieved depending on the molecular architecture and concentration of polymer. Gelation kinetics were not measured quantitatively, but for solutions of 2 cm characteristic lengths, gelation occurred typically in less than a minute. It is believed that gelation rate is heat conduction limited.

The viscoelastic and mechanical properties were evaluated by subjecting the gels at 37 °C to oscillatory stresses (σ) that ranged from 1 to 1000 Pa at 1 Hz frequency and measuring the resulting strains (γ). The elastic modulus (G'), loss modulus (G''), and loss tangent ($\tan \delta \equiv G''/G'$) for the gels within the linear viscoelastic regions are shown in Figure 5a–c. Figure 5d shows the maximum strain vs maximum stress relationship for the gels.

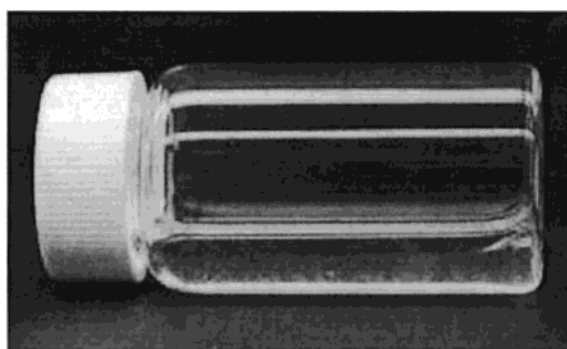
Figure 5a,b shows that for all four gels G' and G'' are approximately constant over a wide range of oscillatory stress values and then decrease sharply at high stress. The stress at which the drops occur are different for the four gels. The G' and G'' values in the constant regions are summarized in Table 3, which shows that G' and G'' increase as the number of arms increase from 1 to 2

to 4 but then decrease upon further branching to an 8-arm architecture. Accordingly, loss tangent for all four gels is also seen to be approximately constant over a wide range of oscillatory stress values but then deviate from linearity at high stress (Figure 5c).

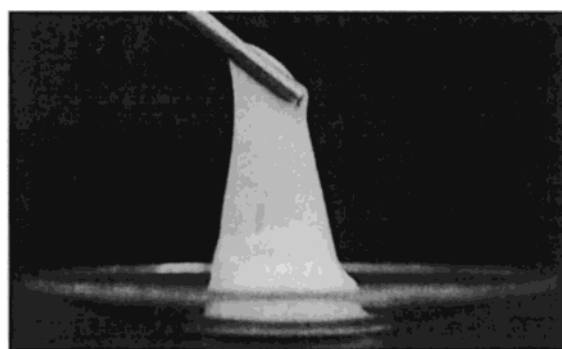
Figure 5d shows that the stress vs strain relationship for all four gels exhibit linear regions, followed by deviations from linearity at high stress and strain values. The linear regions in these curves represent the regions where the overall modulus ($[G'^2 + G''^2]^{1/2}$), rather than just G' or G'' alone, is constant. The corresponding stress and strain at the point where the stress–strain curves begin to deviate from linearity are defined as the yield stress (σ_c), and the critical strain (γ_c), and are summarized in Table 3.

Our hypothesis of the gelation mechanism suggests that multiple PNIPAAm segments are required in the same molecule in order for physically cross-linked hydrogel networks to be formed. Thus, it is expected that the 2-, 4-, and 8-arm structures would form gels via a physical cross-linking mechanism, while the 1-arm diblock copolymer would form a gel via the micellar aggregation mechanism. Comparison of the rheological results for the 2-, 4-, and 8-arm structures shows that the elastic and loss moduli in the linear viscoelastic region as well as the yield stress and strain are all highest for the 4-arm structure, indicating that the 4-arm copolymer forms gels that are highest in strength as well as deformability. Branching should have two effects on gel rheology. Increasing the number of arms should increase the degree of cross-linking in the gel via the covalent linkage of arms; hence, gel strength should increase. However, as the number of arms increases, aggregation between PNIPAAm blocks within the same molecule becomes increasingly favored over intermolecular aggregation. Since intramolecular aggregation does not contribute to physical cross-linking, the degree of physical cross-linking would decrease as branching increases beyond a certain point. The maximum in gel strength observed for the 4-arm gel may thus be explained by the counterbalancing effects of covalent cross-linking and physical cross-linking. It is also interesting to note that the loss tangent increases monotonically from 0.40 to 0.52 to 0.62 as the degree of branching increases from 2 to 8 arms, indicating that the relative viscous component increases with the degree of branching. It is not yet clear what molecular phenomenon gives rise to this result.

A comparison of the rheological behavior of the one-arm micellar aggregate gels to the multiarm physically



(a) 20 %wt A(B)₄ Solution at 25°C



(b) 20 %wt A(B)₄ Gel at 37°C

Figure 4. Material Images at 25 and 37 °C.

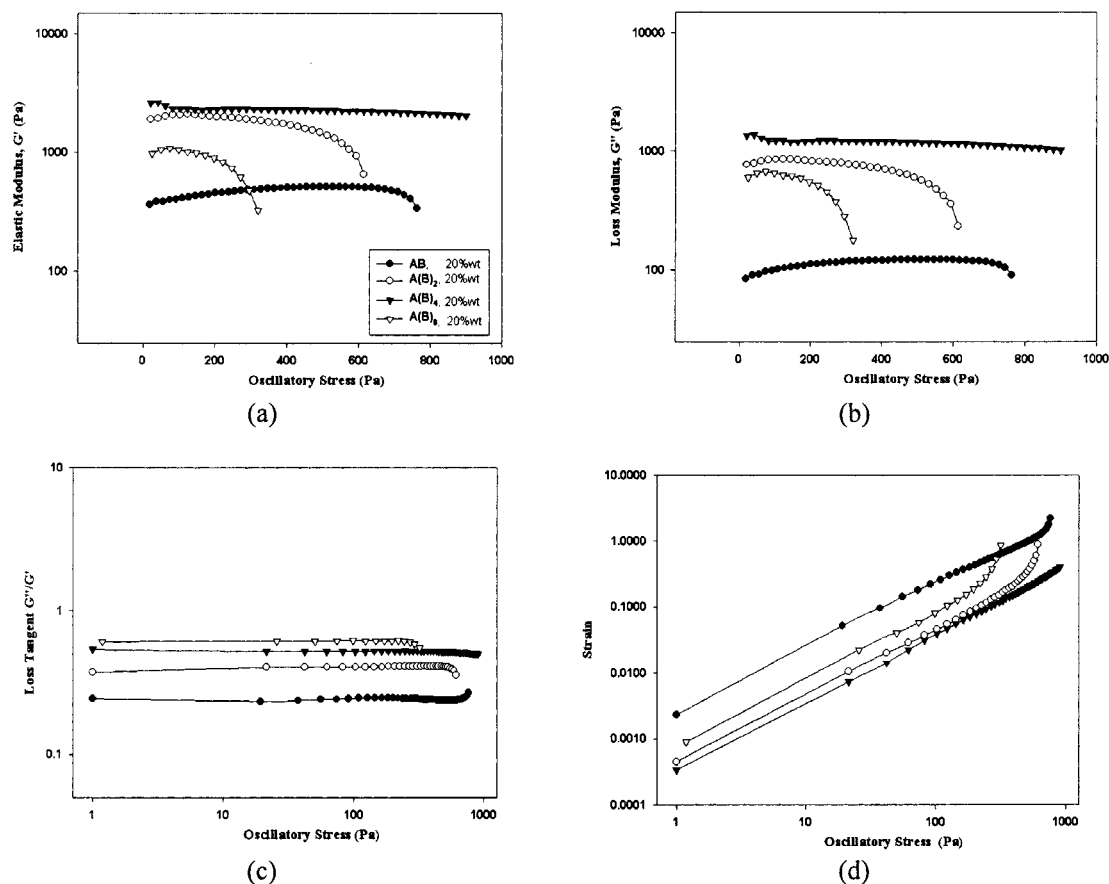


Figure 5. Stress sweep curves of copolymers.

Table 3. Gel Strength of Copolymers at 37 °C^a

materials	G', G'' at linear viscoelastic region		σ_c , yield stress (Pa)	γ_c , critical yield strain
	G' (Pa)	G'' (Pa)		
AB, 20 wt %	480 ± 70	110 ± 20	690 ± 90	1.40 ± 0.15
A(B) ₂ , 20 wt %	2000 ± 200	800 ± 80	430 ± 50	0.24 ± 0.03
A(B) ₄ , 20 wt %	2500 ± 200	1300 ± 100	860 ± 80	0.37 ± 0.04
A(B) ₈ , 20 wt %	1050 ± 150	650 ± 90	200 ± 30	0.19 ± 0.03

^a The G' and G'' values were measured at $\omega = 1$ Hz and $\sigma = 50$ Pa, which is within the linear viscoelastic region of all the materials above. Values are the averages from three synthesis batches.

cross-linked gels shows that the most striking difference between the two classes of gels is that the loss tangent decreases at high stress for the 1-arm gel while for all the other gels loss tangent increases at high stress. The contrast in trends is suggestive of a fundamental difference in the gel structure. The viscous component of the 1-arm gel becomes increasingly dominant at high values of oscillatory stress, while the elastic component of the multiarm gels become increasingly dominant. It is also interesting to note that a well-known micellar aggregate gel composed of Pluronic F98 PEO–PPO–PEO triblock copolymers in water also shows an increasing loss tangent at high stress.²⁵

The 1-arm gel shows a significantly lower values of G' and G'' than the multiarm gels (Table 3). According to Hvidt's classification,^{26,27} the 1-arm gel would be considered a "soft gel" (i.e., $G' < 1000$ Pa), while the others would be considered "hard gels" (i.e., $G' > 1000$ Pa). In contrast to the low modulus, the 1-arm gel has the highest critical strain among the gels and a relatively high yield stress—lower than only the 4-arm gel. With only one end tethered to PNIPAAm aggregates, PEG segments in 1-arm gels are more freely mobile and more readily deformable than PEG segments in multi-

arm gels that are tethered at both ends. The low modulus and high critical strain of the 1-arm gel are a reflection of the ease of deformability. Likewise, with only one end sterically shielded by PNIPAAm aggregates, the free end of PEG segments in 1-arm gels are allowed to interact with other PEG segments and form entanglements. The relatively high yield stress of 1-arm gels may be the result of significant entanglement of PEG corona.

Beside the stress sweep, a frequency sweep from 0.1 to 10 Hz was also performed on each gel at small oscillatory stress of 50 Pa (Figure 6). The modulus of all four gels increases slowly with frequency (ω). It is understood that $G' \sim \omega^{n_1}$ and $G'' \sim \omega^{n_2}$,²⁸ and a low exponent (i.e., $n_1 < 0.5$) usually indicates a highly ordered 3-D structure inside the gel (e.g., a close hard-sphere packing or a rigid continuous network formation).^{29,30} The n_1 exponent determined from a log–log plot of elastic modulus vs frequency was found to be 0.15, 0.19, 0.16, and 0.26 for the 1-, 2-, 4-, and 8-arm gels, respectively ($R^2 > 0.97$ in all cases). All four exponents are of relatively low values. Although this does not help us distinguish between the two hypothesized gelation mechanisms, the low exponents are

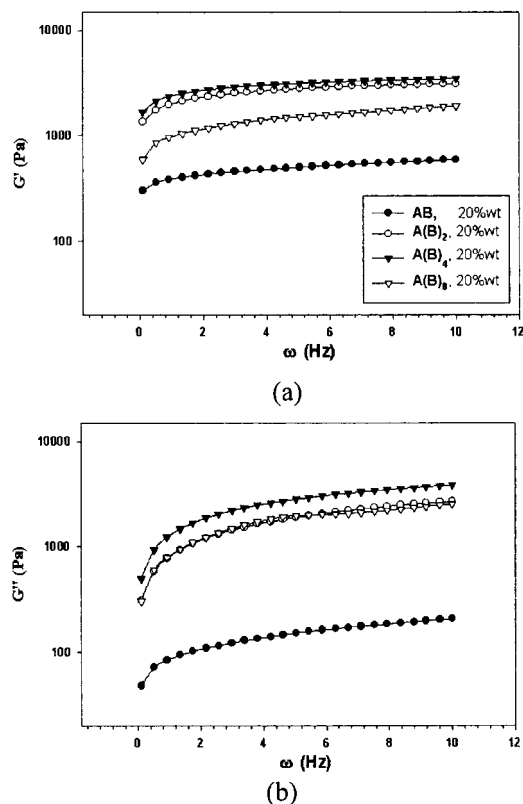


Figure 6. Frequency sweep curves of copolymers.

nevertheless consistent with both close micelle packing for AB gelation and associative network formation for A(B)₂, A(B)₄, and A(B)₈ gelation. The higher exponent of 8-arm gel compared to the rest of three may be an indication of less organized gel structure, consistent with the low yield stress observed for this gel.

Viscosities of PEG–PNIPAAm copolymer solutions were measured at 5 °C and for a shear rate range of 0.1–70 s⁻¹. For a shear rate greater than 5 s⁻¹, all the solutions are essentially Newtonian. The viscosity for 20 wt % a 1-arm diblock, 2-arm triblock, 4-arm star, and 8-arm star are 750, 950, 900, and 700 cP, respectively. All these solutions are of low enough viscosity to easily inject through a 25 G needle.

To study the syneresis of gels, all samples were prepared as 16.7 wt % aqueous solutions and incubated at 37 °C for 2 months. The mass of water squeezed out of the gel during this time was measured. PNIPAAm homopolymer lost about 75% gel mass, whereas PEG–PNIPAAm copolymers only exhibited minimal degree of syneresis. In particular, A(B)₂ and A(B)₄ gels lost less than 5% of gel mass. The low degree of syneresis suggests that the PEG–PNIPAAm copolymer gels have a high degree of equilibrium hydration—a feature that may be useful in some clinical applications.

Conclusions

Block and star copolymers of PEG and PNIPAAm form liquid aqueous solutions at low temperature and

transform to relative strong elastic gels upon heating. Multiple-arm copolymers appear to form gels via a physical cross-linking mechanism, while diblock copolymers gel by a micellar aggregation mechanism. The rheological properties of the gels are dependent on the molecular architecture, with A(B)₄ showing superior properties. The copolymers show low to moderate injection viscosities, high gel strengths, low degrees of syneresis, and rapid gelation kinetics and are therefore promising candidates for clinical uses such as in-situ drug delivery, cell encapsulation, and anatomical barriers.

References and Notes

- (1) De Jong, S. J.; De Smedt, S. C.; Wahls, M. W. C.; Hennink, W. E. *Macromolecules* **2000**, *33*, 3680.
- (2) Nagahara, S.; Matsuda, T. *Polym. Gels Networks* **1996**, *4*, 111.
- (3) Miyata, T.; Asami, N.; Uragami, T. *Macromolecules* **1999**, *32*, 2082.
- (4) Miyata, T.; Asami, N.; Uragami, T. *Nature* **1999**, *399*, 766.
- (5) Petka, W. A.; Harden, J. L.; McGrath, K. P. *Science* **1998**, *281*, 389.
- (6) Cappello, J.; Crissman, J. W.; Crissman, M.; Ferrari, F. A. *J. Controlled Release* **1998**, *53*, 105.
- (7) Jeong, B.; Bae, H. Y.; Lee, D. S.; Kim, S. W. *Nature* **1997**, *338*, 860.
- (8) Jeong, B.; Choi, Y. K.; Bae, Y. H.; Zentner, G.; Kim, S. W. *J. Controlled Release* **1999**, *62*, 109.
- (9) Jeong, B.; Bae, Y. H.; Kim, S. W. *Macromolecules* **1999**, *32*, 7064.
- (10) Jeong, B.; Bae, Y. B.; Kim, S. W. *J. Biomed. Mater. Res.* **2000**, *50*, 171.
- (11) Cabana, A.; Ait-Kadi, A.; Juhasz, J. *J. Colloid Interface Sci.* **1997**, *190*, 307.
- (12) Linse, P.; Malmsten, M. *Macromolecules* **1992**, *25*, 5434.
- (13) US Patent 5759563, Liquid delivery composition, June 2, 1998.
- (14) Royals, M.; Fujita, S. M.; Yewey, G. L.; Dunn, R. L. *J. Biomed. Mater. Res.* **1999**, *45*, 231.
- (15) Yoshioka, H.; Mikami, M.; Mori, Y. *J. Macromol. Sci., Pure Appl. Chem.* **1994**, *A31*, 109.
- (16) Yoshioka, H.; Mikami, M.; Mori, Y. *J. Macromol. Sci., Pure Appl. Chem.* **1994**, *A31*, 113.
- (17) Yoshioka, H.; Mikami, M.; Mori, Y. *J. Macromol. Sci., Pure Appl. Chem.* **1994**, *A31*, 121.
- (18) Kaneko, Y.; Nakamura, S.; Sakai, K.; Aoyagi, T. *Macromolecules* **1998**, *31*, 6099.
- (19) Topp, M.; Dijkstra, P. J.; Talsma, H.; Feijen, J. *Macromolecules* **1997**, *30*, 8518.
- (20) Virtanen, J.; Baron, C.; Tenhu, H. *Macromolecules* **2000**, *33*, 336.
- (21) Shearwater Polymer Inc., In *Catalog of Shearwater Polymer Inc.*, 1999; p 8.
- (22) Mohanty, N.; Pradhan, B.; Mahanta, M. C. *Eur. Polym. J.* **1980**, *16*, 451.
- (23) Smith, G. F. In *Cerate Oxidimetry*; Smith Chemical Co.: Columbus, OH, 1942.
- (24) Sarkar, S. *J. Appl. Polym. Sci.* **1979**, *24*, 1073.
- (25) Lin, H.; Cheng, Y.; Saville, B. A., unpublished data, 2000.
- (26) Hvidt, S.; Jorgensen, E. B. *J. Phys. Chem.* **1994**, *98*, 12320.
- (27) Almgren, M.; Brown, W.; Hvidt, S. *Colloid Polym. Sci.* **1995**, *273*, 2.
- (28) Sahimi, M. In *Application of Percolation Theory*; Taylor and Francis Publisher: London, 1994; Chapter 11, p 176.
- (29) Zhao, J.; Majumdar, B.; Schulz, B.; Mortensen, K. *Macromolecules* **1996**, *29*, 1204.
- (30) Hamley, I. W. In *The Physics of Block Copolymers*; Oxford University Press: Oxford, 1998; Chapter 1.

MA001852M